# Target tracking and classification for missile using interacting multiple model (IMM)

Kyungwoo Yoo and Joohwan Chun
KAIST
School of Electrical Engineering
Yuseong-gu, Daejeon, Republic of Korea
Email: babooovv@kaist.ac.kr

Jinwoo Shin
Agency for Defense Development
Daejeon, Republic of Korea

***Abstract*—To successfully shoot down a flying enemy missile, high accuracy missile tracking is a pre-requisite. However, since the dynamics of the missile change with the phase of the trajectory, there is a limit to the tracking with ordinary Kalman filter (KF) which considers single dynamics. Therefore, in this paper, to improve tracking performance, interacting multiple model (IMM) which considers various dynamic models simultaneously is applied. In addition, by classifying the missile head and debris generated at stage separation using the model probability calculated in the IMM, unnecessary detection and tracking resources used to track debris are reduced. The performance of the proposed method is verified through various simulation results and the favorable results are obtained.**

## I. Introduction

High accuracy missile tracking is essential to shoot down a flying enemy missile successfully. In general, target tracking is performed with a Kalman filter (KF) that considers the dynamics rather than estimating the target with measurements only. However, in the case of missile flying with thrust during a predetermined time according to the missile range and flying through a free fall section without thrust, it is difficult to expect a high tracking performance with a general KF which considers a single dynamic model. One of the well-known methods to solve this problem is the interacting multiple model (IMM) [1], [2], [3], [4]. In order to estimate the target with various dynamics, the IMM performs multiple KFs with various dynamic models at the same time and tracks the target more accurately through weighted average of multiple KF estimates using model probability. There have been many studies on tracking using IMM, and advanced IMM techniques are also being studied [5]. There have also been studies to classify targets with different dynamic characteristics such as drone, civil aircraft and jet [6], [7]. In this study, we propose an algorithm to track missiles and classify the debris that occurs during stage separation. In case of [6], [7], there was a limit in that it takes much time for target classification with high accuracy due to the characteristics of considered target dynamics and the predetermined transition probability used in IMM. However, in this study, we set the new classifier using dynamic characteristics and physical characteristics of the target and using this classifier, classification process is successfully executed in a short time. The paper is composed as follows. Section II and III describe the IMM and dynamic model of the target. In section IV, the target dynamics are analyzed to obtain the dynamic model for IMM. The missile head and debris classification algorithm is described in section V and the performance of the proposed algorithm is verified by various simulations in section VI. Conclusions are given in Section VII.

## II. Interacting multiple model (IMM)

IMM is a method for combining state estimates from multiple filter models to get a better state estimate of target with changing dynamics. Since the IMM is processed based on the KF, we briefly describe the KF before describing the IMM. The dynamic and measurement model of discrete time KF can be expressed as follows.

$$\begin{aligned} x_k &= f\left(x_{k-1}\right) + B_{k-1}u_{k-1} + w_{k-1} \\ z_k &= h\left(x_k\right) + \nu_k \end{aligned} \tag{1}$$

We consider the extended Kalman filter (EKF). $x_k, f\left(\cdot\right), B_{k-1}$ and $u_{k-1}$ are the state variable at time $k$, dynamic model, control input model and control at time $k-1$, respectively. The $w_{k-1}$ is the process noise at time $k-1$ and satifies $w_k \sim \mathcal{N}\left(0, Q\right)$. $z_k, h\left(\cdot\right)$ and $\nu_k$ are the measurement at time $k$, measurement model and measurement noise which satisfies $\nu_k \sim \mathcal{N}\left(0, R\right)$, respectively. Time update and measurement update of EKF can be written as follows.

$$\begin{aligned} \hat{x}_{\,k|k-1} &= f\left(\hat{x}_{\,k-1|k-1}\right) + B_{k-1}u_{k-1} \\ P_{k|k-1} &= F_{k-1}P_{k-1|k-1}F_{k-1}^T + Q \\ e_k &= z_k - h\left(\hat{x}_{\,k|k-1}\right) \\ E_k &= R + H_k P_{k|k-1} H_k^T \\ K_k &= P_{k|k-1}H_k^T E_k^{-1} \\ \hat{x}_{\,k|k} &= \hat{x}_{\,k|k-1} + K_k\left[z_k - h\left(\hat{x}_{\,k|k-1}\right)\right] \\ P_{k|k} &= \left(I - K_k H_k\right) P_{k|k-1} \end{aligned} \tag{2}$$

$\hat{x}_{\,k|k-1}, \hat{x}_{\,k|k}, P_{k|k-1}, P_{k|k}$ are state estimate and covariance of time update and measurement update at time $k$, respectively. $F_{k-1}$ and $H_k$ are Jacobian matrices $F_{k-1} = \left.\frac{\partial f(x_{k-1})}{\partial x_{k-1}}\right|_{x_{k-1}=\hat{x}_{\,k-1|k-1}}, H_k = \left.\frac{\partial h(x_k)}{\partial x_k}\right|_{x_k=\hat{x}_{\,k|k-1}}$.

### A. Compute mixing initial condition and process filter update

Prior to the filter update, the state estimates and covariances of all filters are mixed using mixed model probabilities. If we consider $N$ dynamic models, the mixing initial condition of state estimates and covariances of m-th model at time $k-1$

are calculated as following equation.

$$\begin{aligned}
&\hat{x}^c_{k-1|k-1}(m) \\
&= \sum_{m'=1}^{N} \hat{x}_{k-1|k-1}(m')\,\mu_{k-1|k-1}(m'|\,m), \quad m = 1, ..., N \\
&P^c_{k-1|k-1}(m) \\
&= \sum_{m'=1}^{N} \left( \begin{array}{l} \mu_{k-1|k-1}(m'|\,m) \\ \times \left( \begin{array}{l} P_{k-1|k-1}(m') \\ + \left(\hat{x}^c_{k-1|k-1}(m) - \hat{x}_{k-1|k-1}(m')\right) \\ \times \left(\hat{x}^c_{k-1|k-1}(m) - \hat{x}_{k-1|k-1}(m')\right)^T \end{array} \right) \end{array} \right)
\end{aligned} \tag{3}$$

In the above equation, $\mu_{k-1|k-1}(m'|\,m)$ is $\mu_{k-1|k-1}(m'|\,m) = \frac{p_{m'm}}{\bar{C}_m}\mu_{k-1}(m')$ and $p_{m'm}, \mu_{k-1}(m')$ and $\bar{C}_m$ are model transition probability from $m'$ to $m$ which satisfies $\sum_{m=1}^{N} p_{m'm} = 1$ for all $m'$, model probability of model $m'$ at time $k-1$, $\bar{C}_m = \sum_{m'=1}^{M} p_{m'm}\mu_{k-1}(m')$ respectively. Then, the m-th filter can be updated using mixing initial condition written below.

$$\begin{aligned}
&\hat{x}_{k|k-1}(m) = f\left(m,\ \hat{x}^c_{k-1|k-1}(m)\right) + B_{k-1}u_{k-1}(m) \\
&P_{k|k-1}(m) = F_{k-1}(m)\,P^c_{k-1|k-1}(m)\,F^T_{k-1}(m) + Q_{k-1} \\
&e_k(m) = z_k - h\left(m,\ \hat{x}_{k|k-1}(m)\right) \\
&E_k(m) = R + H_k(m)\,P_{k|k-1}(m)\,H^T_k(m) \\
&K_k(m) = P_{k|k-1}(m)\,H^T_k(m)\,E^{-1}_k(m) \\
&\hat{x}_{k|k}(m) = \hat{x}_{k|k-1}(m) + K_k\left[z_k - h\left(m,\ \hat{x}_{k|k-1}(m)\right)\right] \\
&P_{k|k}(m) = (I - K_k(m)\,H_k(m))\,P_{k|k-1}(m)
\end{aligned} \tag{4}$$

In the above equation, the vector (or matrix) $A(m)$ means $A$ of the m-th filter.

### B. Calculate likelihood function

The likelihood function at model $m$ is obtained through the innovation $e_k(m)$ and innovation covariance $E_k(m)$.

$$\begin{aligned}
&\Lambda_k(m) \\
&= \frac{1}{\sqrt{\det(2\pi E_k(m))}} \exp\left(-\tfrac{1}{2} e^T_k(m)\,E^{-1}_k(m)\,e_k(m)\right)
\end{aligned} \tag{5}$$

Where $\det(\cdot)$ indicates the determinant.

### C. Model probability update

The model probability is obtained by combination of the transition probability, the model probability of the previous time and the likelihood function obtained from the previous step.

$$\begin{aligned}
&\mu_k(m) = \tfrac{\Lambda_k(m)}{C} \sum_{m'=1}^{M} p_{m'm}\mu_{k-1}(m') \\
&\text{where} \quad C = \sum_{m=1}^{M} \left( \Lambda_k(m) \sum_{m'=1}^{M} p_{m'm}\mu_{k-1}(m') \right)
\end{aligned} \tag{6}$$

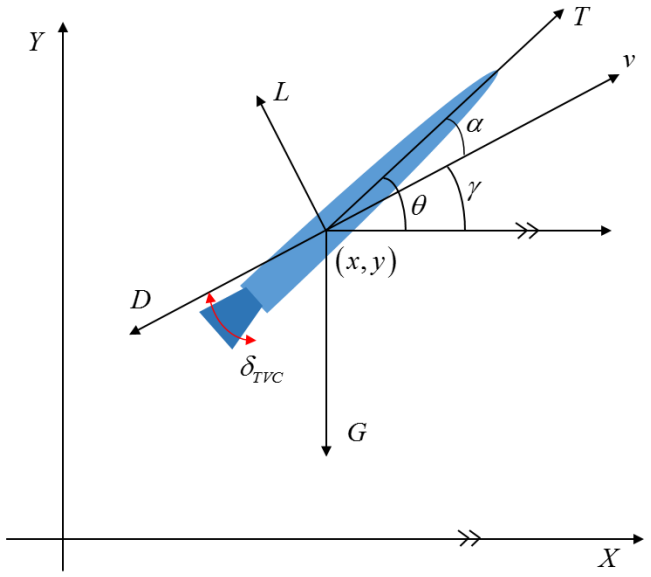


Fig. 1. Missile dynamics

### D. Combine state estimates of multiple filters

In this step, the state estimates are combined by using model probability as follows.

$$\begin{aligned}
&\hat{x}_{k|k} = \sum_{m=1}^{M} \hat{x}_{k|k}(m)\,\mu_k(m) \\
&P_{k|k} = \sum_{m=1}^{M} \left( \mu_k(m) \left( \begin{array}{l} P_{k|k}(m) \\ + \left(\hat{x}_{k|k} - \hat{x}_{k|k}(m)\right) \\ \times \left(\hat{x}_{k|k} - \hat{x}_{k|k}(m)\right)^T \end{array} \right) \right)
\end{aligned} \tag{7}$$

The final state estimates and covariance at time $k$ of IMM becomes $\hat{x}_{k|k}$ and $P_{k|k}$.

## III. Missile Dynamics

In this paper, the missile is considered as a target. We assume missile have two phase which are boost phase and free-fall. The boost phase lasts while the fuel cell (propellant) is burning and the free-fall proceeds after the fuel is exhausted and the fuel cell is separated from the missile. We regard the fuel cell as debris. Fig.1 shows missile states and the force affecting the missile. In the figure above, T, D, L and G are forces caused by thrust, drag, lift and gravity, respectively and the arrows indicate direction of each force. Each force is described as follows [8].

$$\begin{aligned}
T &= I_{sp}\tfrac{W_p}{t_b} \\
D &= \tfrac{1}{2}\rho v^2 c_D s \\
L &= \tfrac{1}{2}\rho v^2 c_L s \\
G &= mg
\end{aligned} \tag{8}$$

The thrust force $T$ is proportional to the amount of fuel cell ($W_p$) and the specific thrust ($I_{sp}$) and occurs until $t_b$ that the fuel cell is exhausted. As the amount of fuel decreases over time, the weight of the missile also decreases. Drag and lift forces are proportional to the square of the target velocity ($v$) and proportional to the surface area of the target ($s$), the atmospheric density ($\rho$) and the lift coefficient ($c_L$)

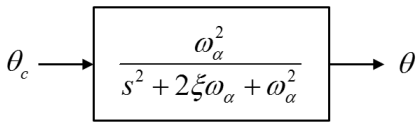


Fig. 2. 2nd-order dynamic model for pitch angle control

related to angle of attack (AoA) and the drag coefficient ($c_D$) related to object shape, respectively. $m$ is weight of target and $g = 9.81m/s^2$. In this study, we consider seven state variables to express missile dynamics, and the equations for each state variable are as follows [8].

$$\begin{aligned}
\dot{v} &= \tfrac{1}{m}\left[T\cos\left(\alpha+\delta_{TVC}\right) - D - G\sin\gamma\right] \\
\dot{\gamma} &= \tfrac{1}{mv}\left[T\sin\left(\alpha+\delta_{TVC}\right) + L - G\cos\gamma\right] \\
\ddot{\theta} &= -T\sin\left(\delta_{TVC}\right)\tfrac{l_{TVC}}{I} \\
\dot{x} &= v\cos\gamma \\
\dot{y} &= v\sin\gamma \\
\dot{\alpha} &= \dot{\theta} - \dot{\gamma} \\
\dot{m} &= -\tfrac{W_p}{t_b}
\end{aligned} \tag{9}$$

In the above equation, $\dot{X}$ and $\ddot{X}$ indicate 1st and 2nd derivative of $X$. $v$, $\gamma$, $\theta$, $x$, $y$, $\alpha$, and $m$ are the velocity, the angle between the ground and the velocity vector of the missile, the angle between the ground and the heading direction (pitch angle), position of the missile (2D), the angle between heading direction and velocity vector (AoA), and the mass of the missile, respectively. $\delta_{TVC}$ is thrust vector control angle through fuel and $I$ represents the moment of inertia. $l_{TVC}$ means control length for thrust vector and is defined as the length from the tail to the center of gravity of the missile. The relationship between the command ($\theta_c$) and response ($\theta$) of the pitch angle is assumed to follow the second-order dynamic model as Fig.2. Therefore, the dynamic equation associated with pitch angle acceleration and the second-order dynamic model can be combined as follows.

$$\begin{aligned}
&\delta_c \simeq \left(2\xi\omega_\alpha\dot{\theta} + \omega_\alpha^2\left(\theta-\theta_c\right)\right)\tfrac{I}{l_{TVC}}\tfrac{1}{T} \\
&where\ \ \delta_{TVC} = \begin{cases} -\delta_{c,\min}, & \delta_c \le -\delta_{c,\min} \\ \delta_c, & -\delta_{c,\min} \le \delta_c \le \delta_{c,\min} \\ \delta_{c,\min}, & \delta_{c,\min} \le \delta_c \end{cases}
\end{aligned} \tag{10}$$

In the above equation, $\delta_{c,\min}$, $\xi$ and $\omega_\alpha$ are set to 5°, 0.93 and 0.5, respectively. Since there is no fuel combustion in the free-fall section, the weight is not reduced. Also, there is no thrust, so the term associated with T is zero. It is also assumed that the posture of missile is stable and the $\alpha$ (AoA) does not change in the free-fall section. Then, the dynamic equations during free-fall section become

$$\begin{aligned}
\dot{v} &= \tfrac{1}{m}\left(D - G\sin\gamma\right) \\
\dot{\gamma} &= \tfrac{1}{mv}\left(L - G\cos\gamma\right) \\
\ddot{\theta} &= 0 \\
\dot{x} &= v\cos\gamma \\
\dot{y} &= v\sin\gamma \\
\dot{\alpha} &= 0 \\
\dot{m} &= 0.
\end{aligned} \tag{11}$$

## IV. Dynamic Model Selection for IMM

In this section, missile dynamics described in section III are analyzed and the dynamic model to be considered at the IMM are set.

TABLE I. Simulation Parameters and Initial States

| Parameter | Value | initial state | Value |
|---|---|---|---|
| $I_{sp}$ | 700 | $v$ | 10m/s |
| $t_b$ | 20sec | $\gamma$ | 68° |
| $C_D\ (=C_{D,mh})$ | 0.4 | $\dot{\theta}$ | $0°/s$ |
| $C_L\ (=C_{L,mh})$ | 0.4 | $x$ | 0m |
| $C_{D,deb}$ | 2 | $y$ | 0m |
| $C_{L,deb}$ | 2 | $\alpha$ | 0° |
| $s\ (=s_{mh})$ | $0.04m^2$ | $m$ | 250kg |
| $l_{TVC}$ | $0.267m$ | | |
| $s_{deb}$ | $0.08m^2$ | | |
| $W_p$ | 150kg | | |
| $\theta_c$ | $\gamma+3°$ | | |

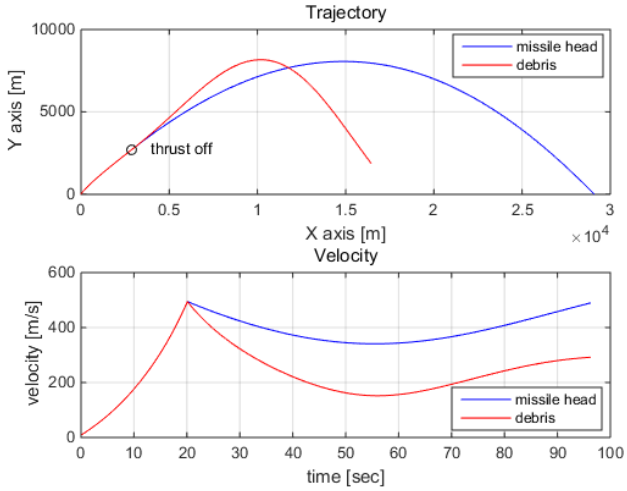


Fig. 3. Trajectory and velocity of missile head and debris

### A. Dynamic analysis

If the fuel cell is separated in the stage separation and divided into several pieces, we can consider each piece as debris which is a plank with curvature. The debris generally receives a larger drag and lift force relatively because of larger drag and lift coefficient and surface area compared to a missile head. To simplify the analysis, in this study, we consider single debris and assume that the weight of the debris is equal to the missile head and the drag and lift coefficient and cross-sectional area of debris are larger than that of missile head. If the missile head and debris have the parameters and initial values as TABLE I, the results of target trajectory and velocity are shown in Fig.3. The missile head's $C_D$, $C_L$ and $s$ ($C_{D,mh}$, $C_{L,mh}$ and $s_{mh}$) are set to same as missile's and the simulation lasted until the missile head fell to the ground. As can be seen from the trajectory graph, both missile head and debris are observed to perform parabolic motion. In the velocity graph, the velocity change suddenly occurs at 20 seconds which is the time when the thrust disappears. In this study, we should know about acceleration characteristics of missile head and the debris since we consider constant velocity (CV) and multiple various acceleration input model as the dynamic model of IMM. The accelerations of the debris and missile head are shown Fig.4. As shown in the simulation results, it is verified that the acceleration varies greatly according to the physical characteristics of objects. We can redraw the results below as x-axis acceleration and y-axis acceleration. In Fig.5, we

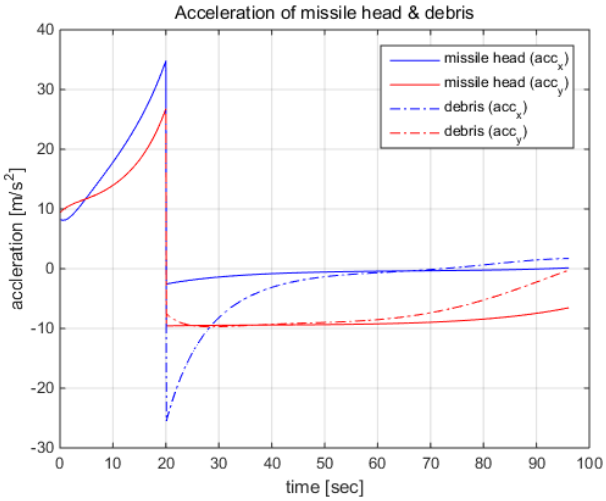


Fig. 4. Accelerations of the debris and missile head

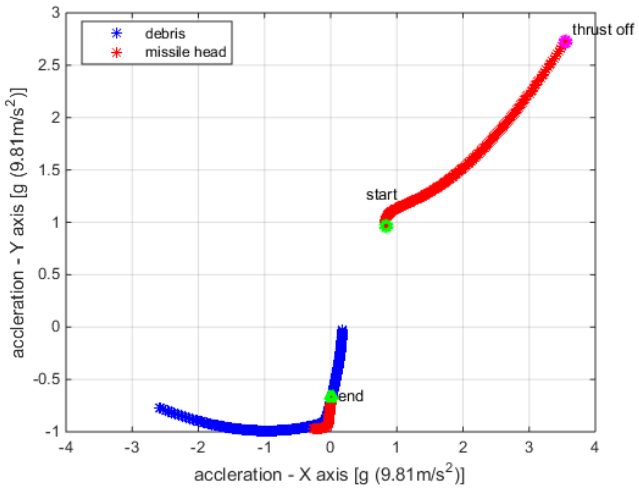


Fig. 5. Accelerations of the debris and missile head (x-y axis)

can know that the missile starts from the starting point and is separated from the thrust off into missile head and debris and has a different acceleration. The unit of each axis is set to $g = 9.81m/s^2$. As shown in the Fig.5, we can see that the acceleration of debris and missile head have different ranges. Based on this results, we select the dynamic model considered in IMM in the next subsection.

### *B. Dynamic model selection for IMM*

As shown in Fig.4 and Fig.5, the acceleration values of missile head and debris during flight are various. However, since IMM cannot establish a dynamic model for all accelerations, we discretize the acceleration as 1g unit for y-axis and 2g unit for x-axis (Because the x-axis acceleration is more widely distributed.). As shown in Fig.6, since the missile head and debris can have a total of eleven acceleration pairs, we determined corresponding 11 acceleration models as dynamic model of IMM. Among the 11 dynamic models, although 1st and 2nd dynamic models are not possible dynamic range for

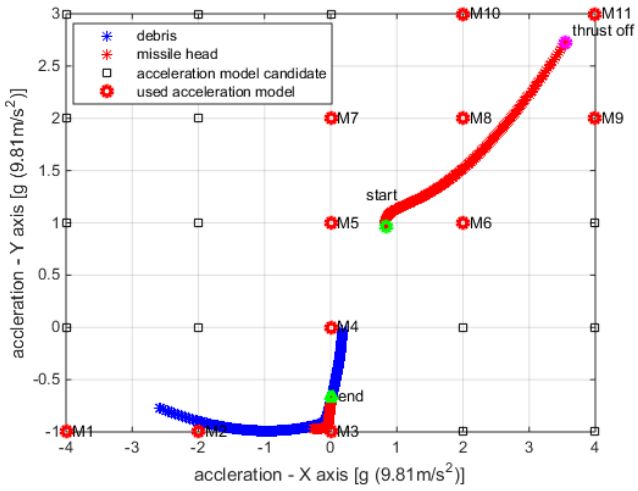


Fig. 6. Discretization of accelerations for IMM

missile head, they are selected for the missile head and debris classification algorithm.

## V. MISSILE HEAD AND DEBRIS CLASSIFICATION ALGORITHM

Since the debris considered in this study occurs after stage separation, single target (missile) is tracked before stage separation. Therefore, we do not need to track two or more targets before the stage separation. That is, what should be preceded by target classification is when the boosting phase finishes and stage separation occurs. Since stage separation occurs at the moment when the thrust disappears, as shown in the preceding acceleration characteristic, it is the same timing as when the dynamic transition occurs from maximum positive acceleration to negative acceleration. In other words, if the value of $\mu_k(3)/\mu_k(11)$ is greater than a predetermined threshold, it can be judged that stage separation has occurred. After the stage separation, more than two measurements are obtained because of the presence of debris. In this study, it is assumed that each measurement is successfully data associated and can be separated for each corresponding target.

Classification method uses 1st and 2nd model probability of IMM, $\mu_k(1)$ and $\mu_k(2)$. In the case of the missile head, $\mu_{k,mh}(1)$ and $\mu_{k,mh}(2)$ are very small during executing IMM since they are not applicable to 1st and 2nd dynamic models, however, in case of debris, $\mu_{k,deb}(1)$ and $\mu_{k,deb}(2)$ are relatively large. Thus we can obtain equation below.

$$\begin{aligned} C_{k,mh} = C_{k,\min} &= \mu_{k,mh}(1) + \mu_{k,mh}(2) \\ &< C_{k,deb} = C_{k,\max} = \mu_{k,deb}(1) + \mu_{k,deb}(2) \end{aligned} \tag{12}$$

In other words, when more than one IMM is executed after a stage separation, only the missile head can be tracked by selecting IMM which has the $C_{k,\min}$. Using above equation we can make threshold $\tau$ which decide whether debris or not as follows.

$$C_k = C_{k,\max}/C_{k,\min} > \tau \tag{13}$$

In this paper, to enhance the classification performance, we revise above equation as shown below.

$$
\begin{aligned}
&C'_k = C'_{k,\max}/C'_{k,\min} > \tau' \\
&where\ C'_{k,\min} = C'_{k,mh} = \frac{\sum_{n=1}^{2} \mu_{k,mh}(n)}{\sum_{n=8}^{11} \mu_{k,mh}(n)}, \\
&C'_{k,\max} = C'_{k,deb} = \frac{\sum_{n=1}^{2} \mu_{k,deb}(n)}{\sum_{n=8}^{11} \mu_{k,deb}(n)}
\end{aligned} \tag{14}
$$

The performances of the above two classifiers are compared in the next section.

## VI. Simulations

Simulation is performed in the same environment as described in TABLE I. The 11 dynamic equations and the measurement equations considered in the IMM are as follows.

$$
\begin{aligned}
\mathbf{x}_{k+1} &= \mathbf{F}\mathbf{x}_k + \Delta t \cdot g \cdot \mathbf{G}\mathbf{u}_k + \mathbf{w}_k \\
\mathbf{z}_{k+1} &= \mathbf{H}\mathbf{x}_{k+1} + \nu_{k+1}
\end{aligned} \tag{15}
$$

In the above equation, $\mathbf{x}_k, \mathbf{F}$ and $\mathbf{G}$ are as follows.

$$
\begin{aligned}
&\mathbf{x}_k = \begin{bmatrix} x_k & v_{x,k} & y_k & v_{y,k} \end{bmatrix}^T, \\
&\mathbf{F} = \begin{bmatrix} 1 & \Delta t & 0 & 0 \\ 0 & 1 & 0 & 0 \\ 0 & 0 & 1 & \Delta t \\ 0 & 0 & 0 & 1 \end{bmatrix}, \ \mathbf{G} = \begin{bmatrix} 0 & 0 \\ 1 & 0 \\ 0 & 0 \\ 0 & 1 \end{bmatrix}
\end{aligned} \tag{16}
$$

The $\Delta t$ is sampling. The covariance of process noise $\mathbf{Q}$ becomes,

$$
\begin{aligned}
&\mathbf{Q} = \mathbf{E}\left[\mathbf{w}_k \mathbf{w}_k^T\right] \\
&= q \begin{bmatrix} (\Delta t)^3/3 & (\Delta t)^2/2 & 0 & 0 \\ (\Delta t)^2/2 & \Delta t & 0 & 0 \\ 0 & 0 & (\Delta t)^3/3 & (\Delta t)^2/2 \\ 0 & 0 & (\Delta t)^2/2 & \Delta t \end{bmatrix} \\
&\mathbf{w}_k = \mathbf{L}\mathbf{n}_k, \mathbf{n}_k \sim \mathcal{N}(0, \mathbf{I}_{4\times 4})
\end{aligned} \tag{17}
$$

where $\mathbf{L}$ is Cholesky decomposition of $\mathbf{Q} = \mathbf{L}\mathbf{L}^\mathbf{T}$. The $\mathbf{u}_k$ has eleven pairs as follows.

$$
\mathbf{u}_k \in \left\{ \begin{matrix} \begin{bmatrix} -4 & -1 \end{bmatrix}^T, \begin{bmatrix} -2 & -1 \end{bmatrix}^T, \begin{bmatrix} 0 & -1 \end{bmatrix}^T, \\ \begin{bmatrix} 0 & 0 \end{bmatrix}^T, \begin{bmatrix} 0 & 1 \end{bmatrix}^T, \begin{bmatrix} 2 & 1 \end{bmatrix}^T, \begin{bmatrix} 0 & 2 \end{bmatrix}^T, \\ \begin{bmatrix} 2 & 2 \end{bmatrix}^T, \begin{bmatrix} 4 & 2 \end{bmatrix}^T, \begin{bmatrix} 2 & 3 \end{bmatrix}^T, \begin{bmatrix} 4 & 3 \end{bmatrix}^T \end{matrix} \right\} \tag{18}
$$

Since we assume that position information is obtained by measurement $\mathbf{z}_{k+1}$, $\mathbf{H}$ and $\nu_{k+1}$ becomes,

$$
\begin{aligned}
&\mathbf{z}_{k+1} = \begin{bmatrix} z_{x,k+1} & z_{y,k+1} \end{bmatrix}^T, \ \mathbf{H} = \begin{bmatrix} 1 & 0 & 0 & 0 \\ 0 & 0 & 1 & 0 \end{bmatrix}, \\
&\nu_{k+1} = \begin{bmatrix} \nu_{x,k+1} & \nu_{y,k+1} \end{bmatrix}^T, \ E\left[\nu_{k+1}{\nu_{k+1}}^H\right] = r \begin{bmatrix} 1 & 0 \\ 0 & 1 \end{bmatrix}
\end{aligned} \tag{19}
$$

The values of $q$ and $r$ are set to 100. In addition, the initial model probability is uniformly set to 1/11 for all models, and

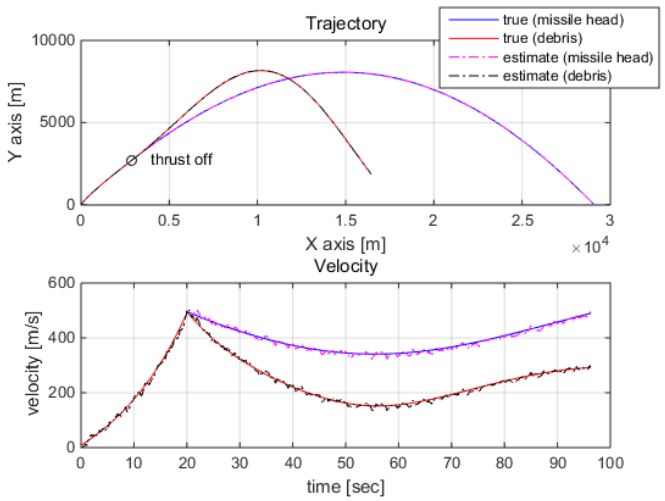


Fig. 7. Estimation results of position and velocity

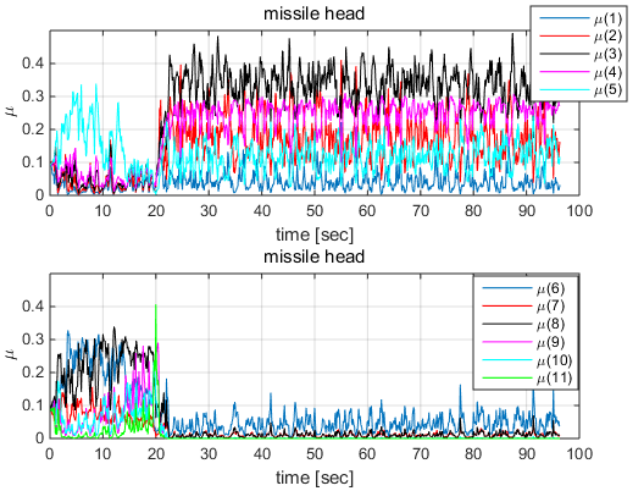


Fig. 8. model probability for missile head

the transition probability for eleven models is set as follows.

$$
p = \begin{bmatrix}
0.9 & 0.1 & 0 & 0 & 0 & 0 & 0 & 0 & 0 & 0 & 0 \\
\frac{0.1}{2} & 0.9 & \frac{0.1}{2} & 0 & 0 & 0 & 0 & 0 & 0 & 0 & 0 \\
0 & \frac{0.1}{2} & 0.9 & \frac{0.1}{2} & 0 & 0 & 0 & 0 & 0 & 0 & 0 \\
0 & 0 & \frac{0.1}{2} & 0.9 & \frac{0.1}{2} & 0 & 0 & 0 & 0 & 0 & 0 \\
0 & 0 & 0 & \frac{0.1}{6} & 0.9 & \frac{0.4}{6} & \frac{0.1}{6} & 0 & 0 & 0 & 0 \\
0 & 0 & 0 & 0 & \frac{0.1}{2} & 0.9 & 0 & \frac{0.1}{2} & 0 & 0 & 0 \\
0 & 0 & 0 & 0 & \frac{0.1}{2} & 0 & 0.9 & \frac{0.1}{2} & 0 & 0 & 0 \\
0 & 0 & 0 & 0 & 0 & \frac{0.1}{4} & \frac{0.1}{4} & 0.9 & \frac{0.1}{4} & \frac{0.1}{4} & 0 \\
\frac{0.1}{6} & \frac{0.1}{6} & \frac{0.1}{6} & \frac{0.1}{6} & 0 & 0 & 0 & \frac{0.1}{6} & 0.9 & 0 & \frac{0.1}{6} \\
\frac{0.1}{6} & \frac{0.1}{6} & \frac{0.1}{6} & \frac{0.1}{6} & 0 & 0 & 0 & \frac{0.1}{6} & 0 & 0.9 & \frac{0.1}{6} \\
\frac{0.1}{6} & \frac{0.1}{6} & \frac{0.1}{6} & \frac{0.1}{6} & 0 & 0 & 0 & 0 & \frac{0.1}{6} & \frac{0.1}{6} & 0.9
\end{bmatrix} \tag{20}
$$

First, to verify the performance of the IMM, we demonstrate the estimated position, velocity, and model probability. As can be seen in Fig.7 and Fig.8, the position and velocity were well estimated, and the tendency of the model probability changed over 20 seconds corresponding to the

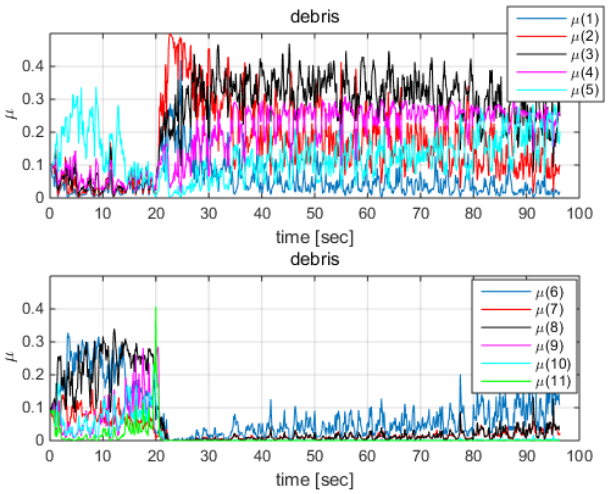


Fig. 9. model probability for debris

TABLE II. RESULTS OF RMSE W.R.T FILTER TYPE

| filter type | RMSE - X [m] | RMSE - Y [m] |
|---|---|---|
| IMM | 4.33 | 4.60 |
| M1 | 12.58 | 5.67 |
| M4 | 4.84 | 5.11 |
| M11 | 11.05 | 10.53 |

stage separation time. TABLE II shows the RMSE of x and y estimates obtained by 1000 Monte-Carlo simulations in case of missile head to compare the tracking performance when IMM and single KF are applied respectively. The RMSE of the IMM is lower than that of the single KF considering only the 1st, 4th (CV ; Constant velocity model) and 11th dynamic models. Among the single KF, M4 (CV) has the smallest RMSE. Fig.10 shows the $C_k$ and $C'_k$ results of missile head and debris when the drag and lift coefficient and cross-sectional area of debris are $(C_{D,deb}, C_{L,deb}, s_{deb}) = [(2C_{D,mh}, 2C_{L,mh}, 2s_{mh}), (5C_{D,mh}, 5C_{L,mh}, 2s_{mh})]$. The number $abc$ in the legend after - in Fig.10 means the case $(aC_{D,mh}, bC_{L,mh}, cs_{mh})$. Simulation results show that $C'_k$

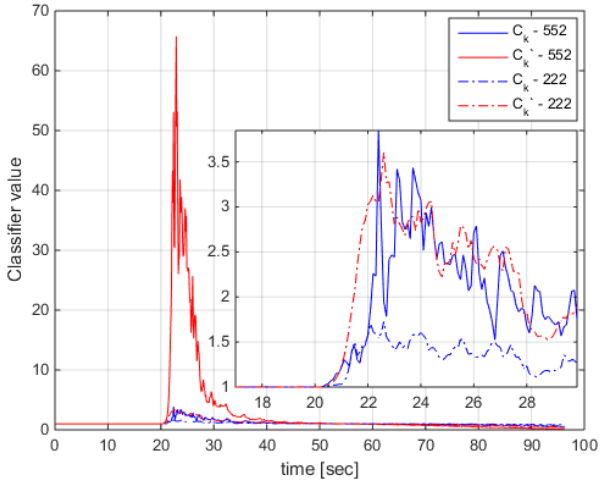


Fig. 10. Comparison of classifier w.r.t debris physical characteristics

TABLE III. RESULTS OF $P_{cs}$ AND $T_c$ ACCORDING TO CLASSIFIER AND DEBRIS PHSICAL CHARACTERISTICS $(a, b, c)$

| debris physical characteristics | $C_k$ | | $C'_k$ | |
|---|---|---|---|---|
| $(a, b, c)$ | $P_{cs}$ | $T_c$ $[sec]$ | $P_{cs}$ | $T_c$ $[sec]$ |
| $(2, 2, 2)$ | 0.99 | 2.48 | 1 | 1.37 |
| $(5, 5, 2)$ | 1 | 1.53 | 1 | 0.94 |

has better discrimination between missile head and debris than $C_k$. In addition, as the physical characteristic difference between missile head and debris increases, the classifier value also increases. TABLE III shows the results of classification success probability $P_{cs}$ and averaging classification time $T_c$ when 1000 Monte-Carlo simulations were performed. Threshold $\tau$ and $\tau'$ is set to 1.5. As can be seen in TABLE III, $C'_k$ has better classification performance than $C_k$ in both debris physical characteristic $(2, 2, 2)$ and $(5, 5, 2)$.

## VII. CONCLUSION

In this study, we track the missile that changes dynamics by using IMM and show better tracking performance than KF using single dynamic model. We also classify missile head and debris with different dynamic characteristics through IMM model probability. Although the amount of computation has been increased slightly by adding additional dynamics to the IMM that the missile head cannot have in order to classify missile head and debris, missile head and debris can be classified within a few seconds through the proposed algorithm. It is expected that it will gain a great benefit in terms of resource management by eliminating the need for unnecessary tracking in a tracking system that uses sensors such as radar.

## REFERENCES

[1] Y. Bar-Shalom, K. Chang, and H. A. Blom, "Tracking a maneuvering target using input estimation versus the interacting multiple model algorithm," *IEEE Transactions on Aerospace and Electronic Systems*, vol. 25, no. 2, pp. 296–300, 1989.

[2] A. F. Genovese, "The interacting multiple model algorithm for accurate state estimation of maneuvering targets," *Johns Hopkins APL technical digest*, vol. 22, no. 4, pp. 614–623, 2001.

[3] W. J. Farrell, "Interacting multiple model filter for tactical ballistic missile tracking," *IEEE Transactions on Aerospace and Electronic Systems*, vol. 44, no. 2, 2008.

[4] S. M. Aly, R. El Fouly, and H. Braka, "Extended kalman filtering and interacting multiple model for tracking maneuvering targets in sensor netwotrks," in *Intelligent solutions in embedded systems, 2009 seventh workshop on*. IEEE, 2009, pp. 149–156.

[5] W. Zhu, W. Wang, and G. Yuan, "An improved interacting multiple model filtering algorithm based on the cubature kalman filter for maneuvering target tracking," *Sensors*, vol. 16, no. 6, p. 805, 2016.

[6] S. Challa and G. W. Pulford, "Joint target tracking and classification," in *Proc. 5th Int. Conf. on Radar Systems (Radar99)*, 1999.

[7] B. Ristic, N. Gordon, and A. Bessell, "On target classification using kinematic data," *Information fusion*, vol. 5, no. 1, pp. 15–21, 2004.

[8] G. M. Siouris, "The generalized missile equations of motion," *Missile Guidance and Control Systems*, pp. 15–51, 2004.